UNIVERSITY OF BIRMINGHAM

Research at Birmingham

The effect of receiver geometry on the optical performance of a small-scale solar cavity receiver for parabolic dish applications

Daabo, Ahmed; Mahmoud, Saad; Al-Dadah, Raya

Link to publication on Research at Birmingham portal

The effect of receiver geometry on the optical performance of a small-scale solar cavity receiver for parabolic dish applications

Ahmed M. Daabo[a,b*], Saad Mahmoud[a], Raya K. Al-Dadah[a]

[a] The University of Birmingham, School of Engineering,
Edgbaston, Birmingham, B15-2TT, UK
[*] Email: axd434@bham.ac.uk
[b] The University of Mosul, Mech. Eng. Dept. Iraq

Abstract

Concentrated Solar Power (CSP) can be used as an efficient low cost energy conversion system to produce different types of energy, such as electricity, through the use of concentrated parabolic dish systems. In the study of CSP, most of the researchers focus on the heat losses and their relationships to the receivers' geometries. The present study concentrates on the optical efficiency as well as the flux distribution of the three different geometries: cylindrical, conical and spherical, of a cavity receiver, with the objective of analysing their behaviour using an advanced ray tracing method.

The results of this study have shown that there is a connection between the flux distribution on the internal surfaces of the cavities and their optical efficiency. Moreover, the conical shape receiver received, as well as absorbed, a higher amount of reflected flux energy than the other shapes. The optical efficiency reached 75.3%, 70.1% and 71.5% for the conical, spherical and cylindrical shapes respectively at surface absorptivity of 85%. Also, the focal point location depends on the shape of the cavity receiver and its absorptivity. Thereby, there is an optimum distance for each design depending on these two factors. The results of the simulated work are validated using the experimental work found in the literature.

Keywords: Concentrated solar plant, Parabolic dish, Cavity receiver, Ray-tracing, Optical efficiency.

1- Introduction

Currently, several countries are increasing the amount of their renewable power plants to produce energy efficiently and to decrease energy consumption. In CSP, most of the researchers concentrate on the heat losses and their relationships to the receivers' shapes; and so the receivers are evaluated depending on their thermal efficiency. They often neglect the amount of heat gain from the receivers' geometries, which helps to increase the heat transfer to the working fluid. Recently, many studies have been conducted on solar tower systems [5- 7], Stirling engines [8, 9], Fresnel lenses [10-12] and solar Brayton cycle enhancement [13-15]. Furthermore, several studies on the heat losses and the receivers' geometries, dimensions and positions are found in [16-23]. For instance, the combined convection and radiation of a modified hemispherical cavity receiver with fins used with solar parabolic dish was numerically analysed by Ngo et al. [16]. Their results showed that the convection heat loss is greatly influenced by the fins' number and receiver's inclination. The radiation loss, on the other hand, is affected by the surface properties of the cavity receiver. The influence of rotation on convection in a rotating cavity receiver for parabolic dish applications was reported in [17]. Abbasi-Shavazia et al. [18] analysed experimentally the heat losses from a cylindrically shaped solar cavity receiver for parabolic dish application at two opening ratios and inclinations ranging from 0[o] to 90[o]. Their results showed that the temperature distribution of the receiver's cavity wall depends on the cavity inclination. Moreover, for the same given total heat input, the region closer to the cavity aperture experienced larger view factors and as a result, larger radiation loss. The thermal performance of multi-cavity concentration was analysed by Austin et al [19]. Intensive studies on the

thermal analysis of cavity receivers for parabolic dish application were achieved by Reddy and Kumar [20-23]. For example, in [21] they studied numerically the influence of both the receiver shape and the receiver orientation of the solar dish concentrator on the convection heat loss. The three configurations are cavity receiver, semi-cavity receiver and modified cavity receiver. The results showed that the convection heat loss in the modified receiver was only about a quarter of the convection heat loss value of the cavity for each 0° and 90° angles. Furthermore, they found that for the modified receiver, the minimum natural convection heat loss at an optimum Aw/A1 was equal to 8. The same researchers [23] investigated the effect of surface emissivity, operating temperature and the orientation of modified receiver geometry for a solar parabolic dish collector on the amount of heat losses. The results revealed that the receiver emissivity has a slight effect on the convective heat losses; whereas its impact on the radiative Nusselt number and radiative loss was very high.

However, there is still some continuing research regarding optical characterisation, even though these studies are in fact for other kinds of solar receivers. For instance, the effects of the concentration ratio on three types of reflective concentrator solar collectors as well as two types of refractive concentrator solar collectors has been investigated numerically by Algarue et al [24]. Their results showed that the optical efficiency for all collectors is about 80% when the concentration ratios are up to 10X. Enhancing the flux distribution of a cylindrical cavity receiver by exploiting the dead space, the area which cannot be coiled by the absorber tube, was achieved by Fuqiang et al. [25]. Two different techniques were used; the first was by changing the height of the interior convex surface and the second was combining the cylindrical receiver with a conical shape at the dead area. Some improvement on the optical efficiency can be achieved during the changing of the dimensions of the interior vortex shape which can cover the dead area. Abdullahi et al. [26] studied single and double elliptical pipe receivers coupled with a compound parabolic concentrator with the previously mentioned type of receiver at different configurations. The results indicated that the optical efficiency of a vertical and horizontal double receiver is greater than the single receiver by 17% and 15%, respectively. The effect of different parameters, such as the parabolic contractor shape, reflectivity, diameter and rim angle, as well as concentrator optical error and solar tracking error have been intensively investigated by Roux et al. [27]. Their results showed that the optimum area ratio depends directly on both tracking and optical errors. Also, the receiver efficiency can be raised up by increasing the dish reflectivity and the precision of both the optics and dish surface. The optical properties of an air tube cylindrical cavity receiver using coupled Monte-Carlo algorithm simulation and five lamps of Xe-arc as a light source were analysed by Qiu et al [28]. Their results revealed that at 300 kW/m^2 average fluxes and 5 m^3/h volume flow rate of air and the maximum outlet temperature reached up to 800°C. Also, they concluded that up to 12% in thermal efficiency of the receiver can be achieved by decreasing the tube diameter from 6 to 4 mm. The improvement of the thermal performance of a solar receiver by focusing on the optical characteristics was studied by Weinstein et al [29]. In their research they aimed to decrease the radiative heat losses, by applying the directional selectivity idea; which led to a reduction in the mentioned heat loss by 75% and as a result achieves high receiver efficiency for solar thermal applications.

To the best of the authors' knowledge, no work has been published on the surface properties of cavity receivers which have significant impact on the thermal performance of the receiver and the system's efficiency. Therefore, this paper tries to focus on the optical efficiency of three different geometries, cylindrical, conical and spherical, of cavity receivers; with the aim of finding the geometry factors and at the same time the properties that can improve it. Using advanced ray tracing (OptisWorks®2012) simulation, the solar ray distribution inside these cavity receiver geometries was investigated at various geometry positions, with respect to the focal point and various values of reflectivity as well.

2- Methodology

Figure (1) shows the three receiver cavities and the parabolic concentrator drawn using SOLIDWORKS® 2015. These three geometries have the same aperture and internal surface areas. The dimensions for the parabolic concentrator and each of the three studied geometries are provided in Table (1). OptisWorks® 2012 an advanced ray tracing software was used to predict the received energy by each surface. More detail about this software is discussed in section 6. This software employs Monte- Carlo algorithm in its analysis as it is a well-known methodology for robust simulation. This method assumes that a large number of rays are going to take their own random paths when they hit the surfaces. Each of the single rays transmits the same amount of energy and has a certain direction which is already determined from the appropriate probability density function. Depending on the surface properties (emissivity, reflectivity and absorptivity) each of these rays will take a specific path which is specified by a set of statistical relationships.

All the studies mentioned previously have used 2D analyses, which record the energy amount that passes through a 2D plane. The weakness of this type of analysis is that it cannot accurately simulate the energy received by 3D geometries as it is only read the energy that passes through the aperture area of each receiver shape and thereby the values of this energy will be almost equal. OptisWorks® 2012 offers the facility of using 3D detectors which are able to read precisely the flux values at every single point; thus the effect of the geometry is highlighted as a main factor, in terms of both the amount of received flux and the distribution. The receiver's shape, the receiver's focal plane position as well as the receiver's wall absorptivity, are examined based on the ratio of received flux and the absorbed flux with respect to the lost energy.

3- Design of the parabolic concentrator

The parabolic concentrator was chosen with a 1m diameter and 45° rim angle, as it gives the maximum concentration ratio [30] as shown in (Fig. 2a). Moreover, it gives the highest amount of received flux among the other rim angles examined; this will be discussed later in this study. (Fig. 2b) and (Fig. 2c) illustrate the relationship between the geometrical dimensions. The focal length can be calculated using Equations (1-3) [30].

$$h = \frac{d^2}{16f} \tag{1}$$

$$\frac{f}{d} = \frac{1}{4\tan\left(\frac{\Psi_{rim}}{2}\right)} \tag{2}$$

$$p = \frac{2f}{1 + cos\Psi_{rim}} \tag{3}$$

Where, h, d, f, Ψ_{rim} and p are the maximum distance (depth) between the vertex and a line drawn across the aperture of the parabola, the aperture diameter, the focal length, parabolic rim angle and parabolic radius respectively.
Also, the rim angle can be determined using Equation (4).

$$\text{Tan } \Psi_{rim} = \frac{1}{\left(d/8h\right) - \left(2h/d\right)} \tag{4}$$

The aperture area of the parabolic dish can be calculated using Equation (5).

$$A_a = \frac{\pi}{4}(2psin\Psi_{rim})^2 \tag{5}$$

Where, $(2psin\Psi_{rim})$ equals the aperture diameter of the parabolic dish.

Equations (3) and (5) can be combined to give Equation (6).

$$A_a = 4\pi\, f^2\, \frac{sin^2\Psi_{rim}}{(1 + cos\Psi_{rim})^2} \tag{6}$$

By considering the origin to be at the vertex V and Y- axis along the axis of the parabola the drawn parabolic concentrator was guided by Equation (7).

$$Y = \frac{X^2}{4f} \tag{7}$$

4- Optical losses

Optical losses are mainly associated with either manufacturing and construction imperfection or material properties. Based on the literature found in [31-35], the types of losses can be summarised as follows:

- Spillage losses are part of radiation hitting outside the aperture of the receiver which can add about 1–3% to the loss.
- Shading losses are related to the ratio of the reflective area of the dish which is shadowed by the receiver. However, this type of loss can be minimized if the dish aperture area is considerably larger than the receiver.
- Reflection losses are the difference between energy falling on the concentrator or receiver surface areas and reflected energy. Depending on the material properties, this loss can represent about 6 to10% from the incoming or received energy.
- Transmission losses can be defined as the amount of energy which is lost in the air when it moves from the concentrator to the receiver; which can add about 2 to 4 % to the loss.
- Absorption losses are the incoming or received energy that can be absorbed by the parabolic concentrator material or the receiver material respectively, which causes thermal stresses.

All these losses have been taken into account in the analysis to evaluate the optical performance of the three investigated geometries. Losses due to errors, like those of structure, tracking, alignment and sensors were not included here. The optical efficiency of the parabolic concentrator can be expressed using Equation (8); whereas the optical efficiency of the receiver can be determined using Equation (9):

$$\eta_{oConc} = \frac{Q_r}{Q_s} \tag{8}$$

Where Q_r, is the energy reaching the receiver's aperture and Q_s is the incident energy through the parabolic concentrator's aperture when it falls on the parabolic concentrator's aperture.

$$\eta_{oRec} = \frac{Q_u}{Q_{rec}} \tag{9}$$

In this case, Q_u is the useful energy that is delivered to the working fluid; whereas Q_{rec} is the amount of energy which is received by the receiver's aperture. It is known that Q_{rec} has a different value from Q_r because sometimes not all the energy that leaves the parabolic concentrator will reach the receiver.

5- Cavity receiver's design

In CSP the main component is the receiver that works as a connection link between the incoming energy (concentrated and reflected by the parabolic dish) and the working fluid inside the receiver. The latter delivers the energy to the system that will convert it into the required form of heat or kinetic energy. Thus the need for an efficient receiver is in great demand by the researchers. One of the main factors regarding the receiver is its size; it should be as small as possible in order to reduce the heat losses [30]. The three investigated geometries were drawn using SOLIDWORKS® 2015. During comparisons, the geometry of each cavity receiver has the same surface and aperture areas (meet the two conditions as the same time). There are two types of concentration ratio [30]: the geometric concentration ratio, which is simply defined as the parabolic concentrator aperture area divided by the receiver surface area; and the optical concentration ratio, which is the averaged flux received by the receiver over the average flux that incident on the area of the parabolic concentrator. In this work the geometric concentration ratio was chosen to be only 5X and the optical ratio ranged from (25X to 30X) depending on the receivers' surface properties.

6- Numerical simulation of the models

OptisWorks® 2012 is commercial software used to simulate the optical performance of different concentrator solar systems based on ray-tracing techniques. This tool has intensively used by some researches [36-43]. With the new features especially the three dimensional detector, the software is capable to see exactly what is going inside the geometry of the cavity receiver and how the reflected flux is distributed on the cavity walls. In this work three different geometries of the thermal cavity receiver as shown in Fig. 1 (cylindrical, conical and spherical) are analyzed. The main aim of this simulation is to determine the effect of shapes of the cavity configuration on the received and at the same time lost flux from the receiver. So, each modeled shape has been simulated in OptisWorks® 2012, which is a three dimensional ray tracing technique in order to determine the amount of received flux by the aperture of each receiver using light source acting as the sun. The properties of the parabolic concentrator such as the material type, the reflectivity are defined. The detector that records the amount of incoming flux from the source as well as the reflected flux to the aperture area of the receiver is initiated. The material property of the receiver that located at the focal point, which depends on the rim angle and diameter of the parabolic concentrator, was also defined. Fig. 3 shows the flow chart of simulation set-up in OptisWorks® 2012. Fig. 4 shows the parabolic concentrator coupled with the thermal receiver and both of them under the ray-tracing analysis.

7- Validation

The two types of simulated work using 2D and 3D doctors carried out in this research have been validated against the experimental work found in [43], see Fig. 5. After designing a similar geometry and set up the OptisWorks® software, the results of the both works were compared and good agreement was achieved. The results of the 2D detector were achieved with an optical efficiency deviation of about 7%; while the 3D detector results were closer to the experimental results with a maximum deviation of about 4.5%. Thus the 2D detector overestimated the results compared to the

experimental value; however the 3D detector underestimated the results compared to the experimental work.

8- Results and discussion

8.1- Choosing the parabolic concentrator's rim angle

The influence of the parabolic concentrator's rim angle has been studied in depth in order to discover which exact value of rim angle would receive and at the same time deliver the flux with minimum optical losses. Six values of rim angle, 15°, 30°, 45°, 60°, 75° and 90° for the concentrator were examined in OptisWorks® 2012. Three of them are shown in Fig. 6. It can be seen from this figure that both the incoming and the received flux are in fact influenced by the parabolic concentrator's rim angle. The reason is that the position of the receiver, which depends on this angle, will approach the either the source, where the rim angle equals 30°, or the parabolic concentrator, where the rim angle equals 90°. Both these configurations are affected by the value of the incoming flux. Fig. 7 shows the effect of the parabolic concentrator's rim angle on the amount of reflected rays and flux on the receiver. It can easily be seen how their amount and values, shown in Fig. 6 and Fig. 7 respectively, varied and how the rim angle of 45° was the best among the chosen investigated angles of the parabolic concentrator. As a result, the parabolic concentrator with a rim angle of 45° was chosen for all the following cases, as it gives the highest received flux. The maximum optical efficiency for the parabolic dish was 92.35%. Fig. 8 (a) shows the designed parabolic concentrator shape; and (b) displays an example of the designed parabolic concentrator after selecting to use all of its body as a 3D detector in order to display the amount as well as the flux distribution. From this figure the effect of receiver shadow on the designed parabolic concentrator can be seen.

8.2- Effect of receiver walls' absorptivity

The influence of the absorptivity for the internal wall surfaces of the cavity receivers is assessed based on the received, reflected, absorbed rays. Also, the way that the flux is distributed inside the cavity receivers is discussed using the 3D detector technique that is accessible in new version of OptisWorks® 2012. This 3D detector allows the researchers for observing how the flux is dispersed inside each of the cavity receivers; as a result it can be known where the dead areas and highly concentrated areas inside the cavity.

The two important themes mentioned above are undesired in cavity receivers design because they reduce the receiver's efficiencies (dead areas) and more heat losses as well as increasing the thermal stresses (highly concentrated areas). For instance the highly concentrated areas in the cavity receivers cause hot spots which initiate the material threshold and it may lead to material failure in receiver. The rays as well as the flux distribution for the three geometrical shape including; spherical, conical and cylindrical at different absorptivity values of internal surface are shown in (Figs 9a 9b and 9c) respectively. At this point it is important to highlight that all of the three shapes were investigated at the same focal length and same positions of the cavity receivers. In terms of the amount of reflected rays, it is clear that the amount of reflected rays is directly proportional with to the absorptivity, which is taken into consideration the cavity shape of the receiver. However, those reflected rays are not always considered as energy loss leaving the cavity shape; instead they are influenced by the geometry shape. For example, at 85% absorptivity, the ratio of the rays which are reflected and lost from the cavity is much higher in the spherical geometry compared to the other two shapes (conical and cylindrical). While the minimum loss due to the reflection rays occurred on the conical shape. Furthermore, the flux distribution for each cavity shape was also directly affected by the geometry.

For instance, there is a big difference in the amount of lost rays between the spherical and the cylindrical geometries. It can be seen that when the flux was uniformly distributed in the cylindrical shape, some areas in the spherical geometry were suffering from a lack of flux and at the same time some other areas were highly fluxed. At 75% absorptivity, the scenario is not much different except that the amount of lost reflected rays is higher. For the ideal case of 100% absorptivity, when it is assumed that all the rays which are hitting the cavity geometry are absorbed by its surface, it can be noticed that the geometry has no strong effect on the reflected rays. However, it does have an influence on the ratio of the fluxed area inside each cavity which depends on the position of the ascending rays which coming from the concentrator. So in this case the worst flux distribution was for the spherical cavity where the difference between the highly fluxed areas and those of zero flux is very big.

8.3- Effect of receiver's position

The effect of receiver position with respect to the focal point is intensely investigated. The influence of the cavity shape has also been considered in order to see the performance of rays, and flux distribution, at each cavity configuration and its position. Once more, the 3D detectors assisted the researchers from visualisation the behaviour that the rays follow and at the same time studying their outcomes. (Figs 10a, 10b and 10c) show the results of this effect for the three studied positions for the spherical cavity shape at three different absorptivity; 100%, 85% and 75%, respectively. In (Fig. 10a), where the assumed absorptivity is 100%, the effect of shifting the receiver position, with respect to the focal point can be seen. Where the worst distribution of flux occurred when the focal point was positioned inside the spherical cavity, the best one however is when the geometry was shifted away, to let the focal point located outside the geometry. Similar behaviour can also be noticed when the absorptivity were assumed to be 85% and 75%, (Figs. 10b &10c) respectively. However, the amount of the received flux as well as the areas where most of the flux was concentrated (the tips) for the last two cases, (Fig. 10b) and (Fig.10c), differ from that shown in (Fig. 10a). These areas are the tips of the spherical cavity receiver. In the same way, (Figs 11a, 11b and 11c) show the effect of changing the position of the conical cavity shape receiver with respect to the focal point at three different absorptivity values including; 100%, 85% and 75%, respectively. In (Fig. 11a), where the absorptivity is 100% (black body), the effect of varying the receiver position with respect to the focal point can be observed. The tip area was almost unaffected by changing the receiver position. However the amount of received flux was the highest compared to the other cases in (Figs. 11b &11c). Fig. 11b shows the best flux distribution is when the geometry was shifted towards the concentrator's direction and the focal point was located inside the geometry (at 85% absorptivity). However, this was not the case when the absorptivity was assumed to be 75%, as shown in (Fig. 11c), where better distribution was achieved by shifting away the receiver's position from the concentrator's direction; this allows the focal point to be located outside the geometry. Similarly (Figs 12a, 12b and 12c), display the rays and the flux distribution for the cylindrical cavity receiver. In case of 100% absorptivity, it is clear that the best distribution was realised when the focal point is at the aperture plane. However, this was not always the case when the supposed absorptivity values were considered to be 85% and 75% as shown in (Figs 12b &12c) respectively. In these two figures the best distribution was noticed to be when the receiver geometry shifted away from the concentrator's direction, and the focal point was located outside the receiver geometry. Additionally, an enlarged cross sectional view for the three configurations of the receiver is illustrated in Fig. 13 where the difference in the flux distribution is clear. In the spherical receiver most of the flux comes from the middle of the shape; however, in the other two shapes all the receiver's body may be fluxed.

8.4- Effect of receiver's cavity shape

It is clear that the geometry shape itself has a role in terms of the amount of energy received, absorbed, reflected and lost. After the rays hit the cavity wall they have two different probabilities, either to be directly absorbed by the wall or reflected by the internal cavity surfaces. While the absorbed rays are measured as useful energy, the reflected rays also have two different possibilities. They either hit another part of the cavity surface area and by doing so those rays will have the chance to be absorbed by the internal cavity walls and calculated as useful energy, or they might go directly outside the cavity geometry through the aperture area so they will be considered as lost energy. Therefore the geometry shape of the receiver plays an important role in terms of reflected rays as well as the number of times that these rays are going to be reflected. As a result the influence of the receiver's geometry is investigated in order to know which path each geometry has followed.
From Fig. (14), it is clear that the conical shape has absorbed the highest amount of energy compared to the other two receivers' configurations. However, the maximum energy values absorbed are different for each cavity shape at each proposed receiver absorptivity value. In detail, at 75% absorptivity, the maximum absorbed energy for the spherical, conical and cylindrical shapes were about 349, 375 and 333 watts at 570, 560 and 585 mm respectively. However, these values were about 355, 378 and 360 watts at 565, 555 and 590 mm respectively at 85% absorptivity.

Figure (15) shows the optical efficiency for the three shapes at various focal distances at surface absorptivity of 75% and 85%. It is clear from this figure that the conical receiver cavity has the highest optical efficiency reaching about 75.3% and 72.4% for absorptivity of 85% and 75% respectively. The cylindrical shape achieved the lowest optical efficiency at 75% absorption with an optical efficiency of around 63%; however, at 85% absorption the preference became to the cylindrical receiver. The maximum optical efficiency value of the spherical geometry was about 67%.

Uniformity Factor (UF)

The common methods for calculating the uniformity, such as those which refer to the standard deviation or the method in Equation (10), are useful when 2D planes are analysed. However, as the authors are dealing in this study with 3D geometries, those methods would not be effective. The first one (the method of standard deviation) is too complex and the latter (in Equation 10) would be inaccurate as there are some areas inside the receivers' cavity where their minimum flux is zero. Filipa, [44] used another factor (called 'inhomogeneity', r) which was calculated using Equation (11). However, in this study there are some areas their minimum flux is zero so the results of using that form will be more than unity. Some other equations, which can be used for calculating the uniformity, are found in [45]. Again, those equations cannot be utilized in this study for the same reasons mentioned above.

For the sake of comparison, the illumination uniformity of the receivers is estimated by using a uniformity factor. The maximum flux was determined by considering the highest fluxed areas inside the receivers; while the average irradiance was calculated based on the incoming energy divided by the internal surface area of each cavity. So, to investigate the uniformity of the three studied configurations at the different focal distance values, the Uniformity Factor (UF) can be formatted as shown in Equation (12):

$$U = \frac{Maximum\ Irradiance - Minimum\ Irradiance}{Maximum\ Irradiance + Minimum\ Irradiance} * 100\% \qquad (10)$$

$$r = \frac{Maximum\ Irradiance - Minimum\ Irradiance}{Average\ Irradiance} * 100\% \qquad (11)$$

$$UF = \left[1 - \left(\frac{Maximum\ Irradiance - Average\ Irradiance}{Maximum\ Irradiance}\right)\right] * 100\% \qquad (12)$$

Figure (16) show the variation of the illumination's uniformity factor of the three cavity receiver configurations at different focal distances at surface absorptivity of 85% and 75%. In general the conical receiver demonstrated the highest uniformity of illumination: 77% and 84% among the three receivers along all the focal distances at absorptivity of 85% and 75% respectively. Furthermore, as the focal distance increased to range between 580 and 590 mm, the uniformity of all the three shapes increased; beyond this distance the uniformity started to decrease. The reason for that is when the receiver is located at higher focal distances the diffused rays will accumulate at the focal point and then separate to hit almost all the internal surface areas of the cavity. After a specific focal distance the uniformity became lower. Moreover, it is clear that the uniformity at the absorptivity of 75% is higher because the number of reflected rays is higher; which leads to a stronger possibility of increasing the areas that can be subjected to these reflected rays.

Figure (17) displays the flux distribution of the three receivers' cavities at their highest flux uniformities. The best distribution was achieved at relatively higher focal distance values (where most of the surface area had the same colour) which at the same time demonstrated relatively lower optical efficiencies. The reason for this lower value of efficiency is because of the higher ratio of rays which will be lost (directed outside the shape's aperture).

The main reason for this preference in terms of both the flux uniformity and the value of the optical efficiency is the length of the conical shape, which is the longest length among the other shapes. That length and the convergent nature of the shape, traps most of the rays and makes them release their energy inside the cavity.

9- Conclusions

In this study simulation work using a cavity receiver with three different geometries: cylindrical, conical and spherical, was carried out with the objective of analysing the shapes' behaviour optically using the ray tracing method in OptisWorks® 2012. The results of the simulated work are validated against the experimental work found in the literature. The outcome has been concluded in the following points:

1- The conical shape is able to hold a higher amount of incoming energy, from the concentrator, compared to the other two shapes. The maximum optical efficiency reached 72.2%, 68.7% and 65.4% for the conical, spherical and cylindrical shapes respectively at absorptivity of 75%. The optical efficiency for the whole parabolic dish/receiver system was 66.67%, 63.4 % and 60.4% for the conical, spherical and cylindrical shapes respectively.

2- The optimum location of the focal point changes with respect to the receiver shape, as well as the value of its absorptivity. The maximum energy values were received and absorbed by the conical shape when it was located at 570 mm and 565 mm for 75% and 85% absorptivity respectively; for the spherical shape at 560 mm and 555 mm for 75% and 85% absorptivity respectively; and for the cylindrical shape at 585 mm and 590 mm for 75% and 85% absorptivity respectively. From all the geometrical shapes developed and simulated in this

research work it can be concluded that the cylindrical shape has achieved the best flux distribution.

3- The simulated work was validated against experimental work with a maximum deviation of 7% at 45o and 4.5 % at 15o for the 2D and 3D detectors respectively. The lower deviation of the simulation work compared to the experimental work shows that the simulation was accurate enough to justify the results.

4- The conical shape has the best illumination uniformity of all the investigated focal distance values.

5- In general, the uniformity factor at 75% is higher than the one at lower 85% absorptivity for all the shapes.

References

[1] Thakkar, Vanita, Ankush Doshi, and Akshaykumar Rana. "Performance Analysis Methodology for Parabolic Dish Solar Concentrators for Process Heating Using Thermic Fluid."

[2] Lovegrove, Keith, and Wes Stein, eds. Concentrating solar power technology: principles, developments and applications. Elsevier, 2012.

[3] Jaffe, Leonard D. "Dish concentrators for solar thermal energy." Journal of energy 7.4 (1983): 304-312.

[4] Le Roux, W., T. Bello-Ochende, and J. P. Meyer. "Solar tracking for a parabolic dish used in a solar thermal Brayton cycle." Proceedings of the Postgraduate Symposium. 2012.

[5] Carrizosa, E., et al. "Optimization of multiple receivers solar power tower systems." Energy 90 (2015): 2085-2093.

[6] Piroozmand, Pasha, and Mehrdad Boroushaki. "A computational method for optimal design of the multi-tower heliostat field considering heliostats interactions." Energy 106 (2016): 240-252.

[7] Zhang, Maolong, et al. "Performance of double source boiler with coal-fired and solar power tower heat for supercritical power generating unit." Energy104 (2016): 64-75.

[8] Beltrán-Chacon, Ricardo, et al. "Design and analysis of a dead volume control for a solar Stirling engine with induction generator." Energy 93 (2015): 2593-2603.

[9] Ferreira, Ana C., et al. "Thermodynamic and economic optimization of a solar-powered Stirling engine for micro-cogeneration purposes." Energy 111 (2016): 1-17.

[10] Yeh, Naichia. "Illumination uniformity issue explored via two-stage solar concentrator system based on Fresnel lens and compound flat concentrator." Energy 95 (2016): 542-549.

[11] Bendato, Ilaria, et al. "Stochastic techno-economic assessment based on Monte Carlo simulation and the Response Surface Methodology: The case of an innovative linear Fresnel CSP (concentrated solar power) system."Energy 101 (2016): 309-324.

[12] Hussain, M. Imtiaz, Asma Ali, and Gwi Hyun Lee. "Performance and economic analyses of linear and spot Fresnel lens solar collectors used for greenhouse heating in South Korea." Energy 90 (2015): 1522-1531.

[13] Goodarzi, Mohsen, Mohsen Kiasat, and Ehsan Khalilidehkordi. "Performance analysis of a modified regenerative Brayton and inverse Brayton cycle."Energy 72 (2014): 35-43.

[14] Al-Sulaiman, Fahad A., and Maimoon Atif. "Performance comparison of different supercritical carbon dioxide Brayton cycles integrated with a solar power tower." Energy 82 (2015): 61-71.

[15] E., T. Bello-Ochende, and J. P. Meyer. "Integrated solar thermal Brayton cycles with either one or two regenerative heat exchangers for maximum power output." Energy 86 (2015): 737-748.

[16] Ngo, L. C., Tunde Bello-Ochende, and Josua P. Meyer. "Three-dimensional analysis and numerical optimization of combined natural convection and radiation heat loss in solar cavity receiver with plate fins insert." Energy Conversion and Management 101 (2015): 757-766.

[17] Wu, Wei, et al. "On the influence of rotation on thermal convection in a rotating cavity for solar receiver applications." Applied Thermal Engineering70.1 (2014): 694-704.

[18] Abbasi-Shavazi, E., G. O. Hughes, and J. D. Pye. "Investigation of Heat Loss from a Solar Cavity Receiver." Energy Procedia 69 (2015): 269-278.

[19] Fleming, Austin, et al. "A general method to analyze the thermal performance of multi-cavity concentrating solar power receivers." Solar Energy (2015).

[20] Reddy, K. S., and N. Sendhil Kumar. "Convection and surface radiation heat losses from modified cavity receiver of solar parabolic dish collector with two-stage concentration." Heat and Mass Transfer 45.3 (2009): 363-373.

[21] Kumar, N. Sendhil, and K. S. Reddy. "Comparison of receivers for solar dish collector system." Energy Conversion and Management 49.4 (2008): 812-819.

[22] Reddy, K. S., and N. Sendhil Kumar. "Combined laminar natural convection and surface radiation heat transfer in a modified cavity receiver of solar parabolic dish." International Journal of Thermal Sciences 47.12 (2008): 1647-1657.

[23] Kumar, N. Sendhil, and K. S. Reddy. "Numerical investigation of natural convection heat loss in modified cavity receiver for fuzzy focal solar dish concentrator." Solar Energy 81.7 (2007): 846-855.

[24] A. Algaruea, S. Mahmouda, R.K. AL-Dadah, Optical Performance of Low Concentration Ratio Reflective and Refractive Concentrators for Photovoltaic Applications. Energy Procedia 61 (2014) 2375 – 2378.

[25] Wang, F., Lin, R., Liu, B., Tan, H., & Shuai, Y. (2013). Optical efficiency analysis of cylindrical cavity receiver with bottom surface convex. Solar Energy, 90, 195-204.

[26] B. Abdullahia, R. K. Al-dadaha, S. Mouhmud. Optical Performance of Double Receiver Compound Parabolic Concentrator Energy Procedia 61 (2014) 2625 – 2628.

[27] Le Roux, Willem Gabriel, Tunde Bello-Ochende, and Josua P. Meyer. "The efficiency of an open-cavity tubular solar receiver for a small-scale solar thermal Brayton cycle." Energy Conversion and Management 84 (2014): 457-470.

[28] Qiu, Kunzan, et al. "Simulation and experimental study of an air tube-cavity solar receiver." Energy Conversion and Management 103 (2015): 847-858.

[29] Weinstein, Lee, et al. "Optical cavity for improved performance of solar receivers in solar-thermal systems." Solar Energy 108 (2014): 69-79.

[30] Stine, William B., and Michael Geyer. "Power from the Sun." (2001).

[31] Mancini, Thomas, et al. "Dish-Stirling systems: An overview of development and status." Journal of Solar Energy Engineering 125.2 (2003): 135-151.

[32] Kribus, Abraham, et al. "A miniature concentrating photovoltaic and thermal system." Energy Conversion and Management 47.20 (2006): 3582-3590.

[33] Feuermann, Daniel, and Jeffrey M. Gordon. "High-concentration photovoltaic designs based on miniature parabolic dishes." Solar Energy 70.5 (2001): 423-430.

[34] Alaphilippe, Muriel, Sébastien Bonnet, and Pascal Stouffs. "Low power thermodynamic solar energy conversion: coupling of a parabolic trough concentrator and an Ericsson engine." International Journal of Thermodynamics 10.1 (2007): 37-45.

[35] Segal, Akiba, and Michael Epstein. "Optimized working temperatures of a solar central receiver." Solar Energy 75.6 (2003): 503-510.

[36] Ali, Imhamed M. Saleh, et al. "Optical performance evaluation of a 2-D and 3-D novel hyperboloid solar concentrator." World Renewable Energy Congress XI. 2010.

[37] Arnaoutakis, Georgios E., et al. "Enhanced energy conversion of up-conversion solar cells by the integration of compound parabolic concentrating optics." Solar Energy Materials and Solar Cells 140 (2015): 217-223.

[38] Sellami, Nazmi, and Tapas K. Mallick. "Optical efficiency study of PV crossed compound parabolic concentrator." Applied Energy 102 (2013): 868-876.

[39] Baig, Hasan, et al. "Performance analysis of a dielectric based 3D building integrated concentrating photovoltaic system." Solar Energy 103 (2014): 525-540.

[40] Arnaoutakis, Georgios E., et al. "Coupling of sunlight into optical fibres and spectral dependence for solar energy applications." Solar energy 93 (2013): 235-243.

[41] Sellami, Nazmi, and Tapas K. Mallick. "Optical characterisation and optimisation of a static Window Integrated Concentrating Photovoltaic system." Solar Energy 91 (2013): 273-282.

[42] Ali, Imhamed M. Saleh, et al. "An optical analysis of a static 3-D solar concentrator." Solar Energy 88 (2013): 57-70.

[43] Abdullahi, B., et al. "Optical and thermal performance of double receiver compound parabolic concentrator." Applied Energy 159 (2015): 1-10.

[44] Reis, Filipa. "Development of photovoltaic systems with concentration." (2013).

[45] Moreno, Ivan. "Illumination uniformity assessment based on human vision."Optics letters 35.23 (2010): 4030-4032.
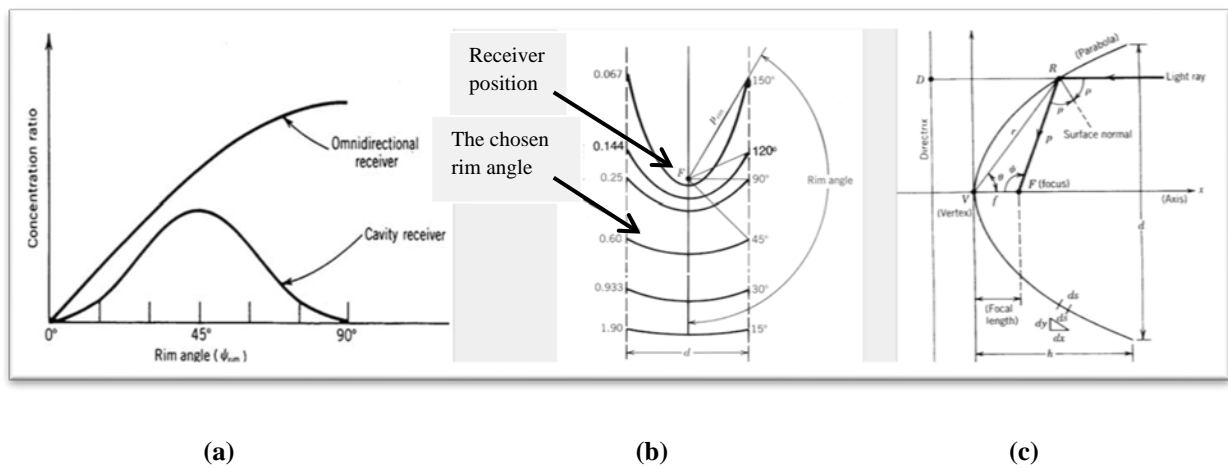
Nomenclature

A: Area   (m^2)
Aa: Aperture area   (m^2)
D: Diameter   (m)
ED: External Diameter   (m)
F: Focal point   (-)
H: Height of receiver   (m)
T: Thickness   (m)
η_o: Optical efficiency   (-)

Subscripts

Con: Conical,
Cyl: Cylindrical
Sph: Spherical
r : Received
Rec: Receiver
Conc: Parabolic Concentrator

(a)

(b)
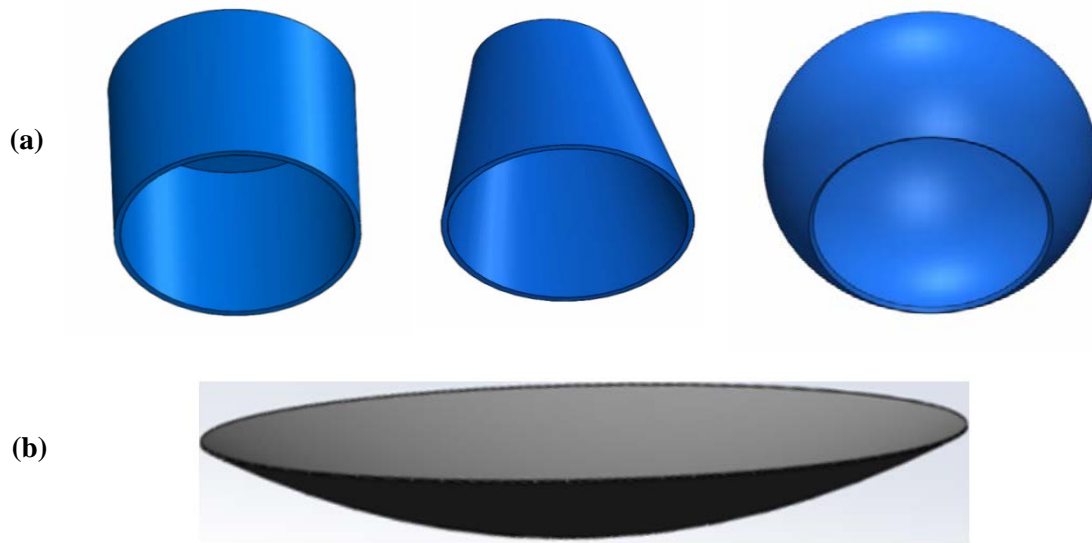
Fig.1. (a): The three geometry shapes of cavity receiver s and (b): The parabolic concentrator dish.

(a)   (b)   (c)

Fig. 2(a): The relationship between the geometrical concentration ratio and rim angle; (b): Segments of a parabola with typical focus F and the identical aperture diameter; and (c): Segments of a parabola.
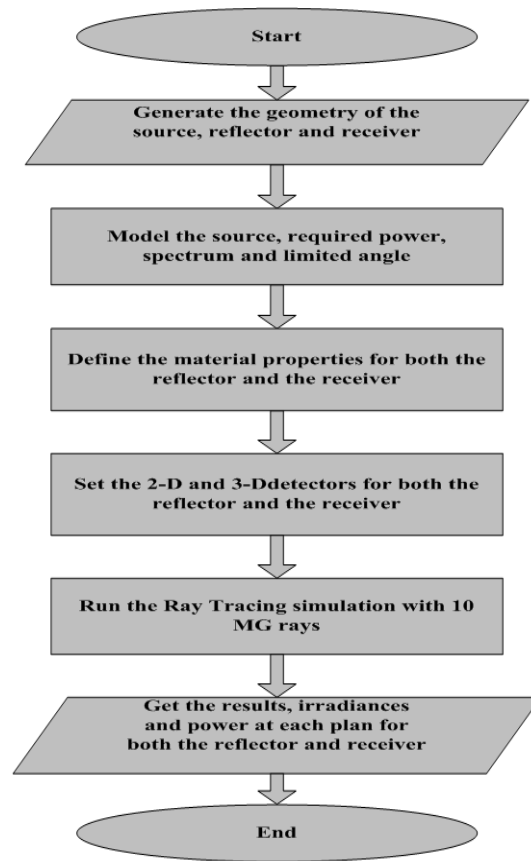
Fig. 3. Flow chart of modelling process of parapolic parabolic concentrator and receiver using ray tracing technique.

(a)   **(b)**
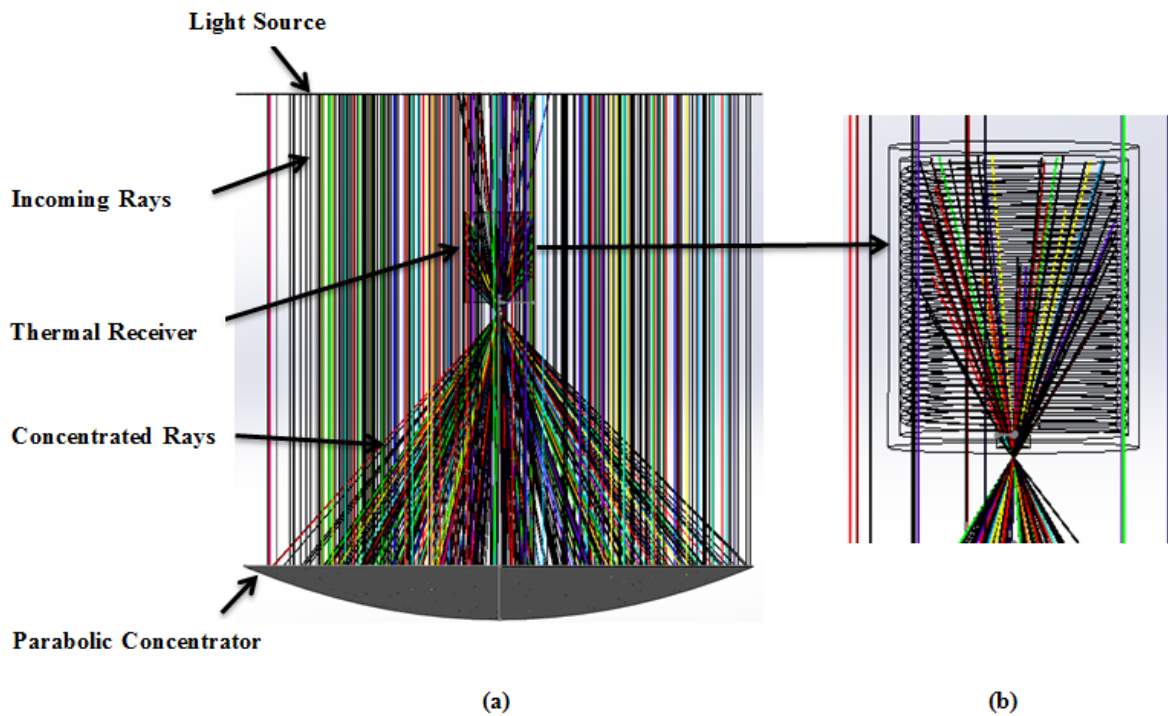
Fig. 4. OptisWorks$^{\circledR}$ simulation (a): Parabolic concentrator with receiver and (b): Cylindrical receiver.
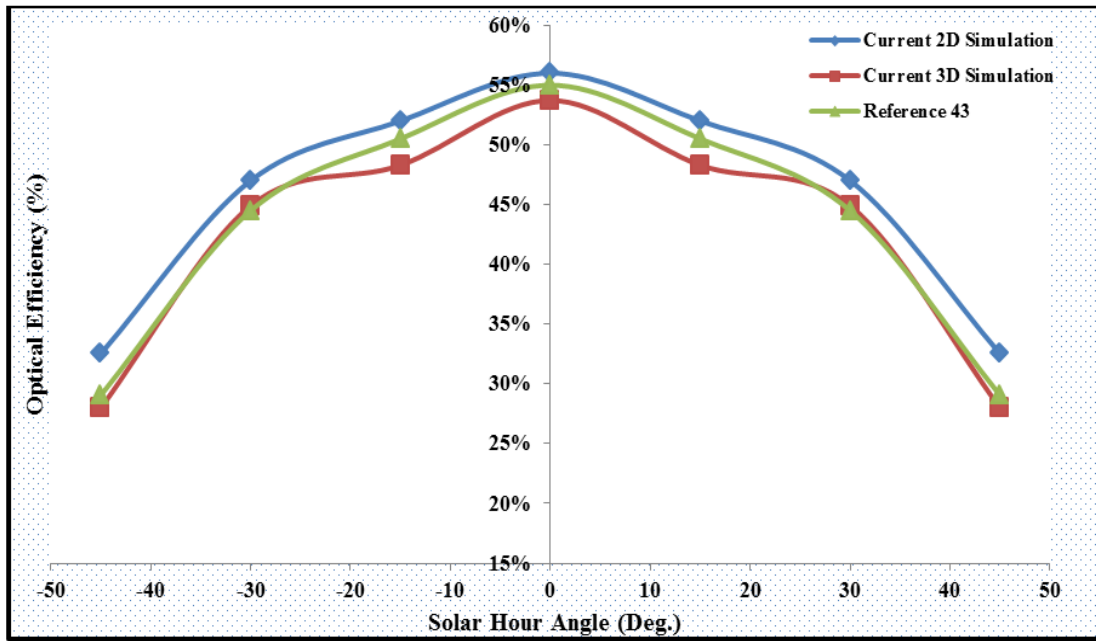
Fig. 5. Comparison of the whole system's optical efficiency from the current study and Ref. [43].

| 30° | 45° | 90° |
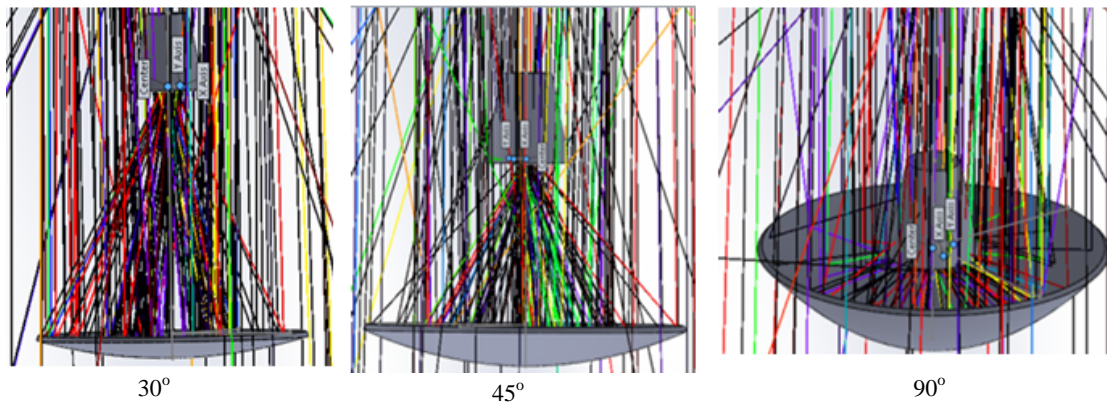
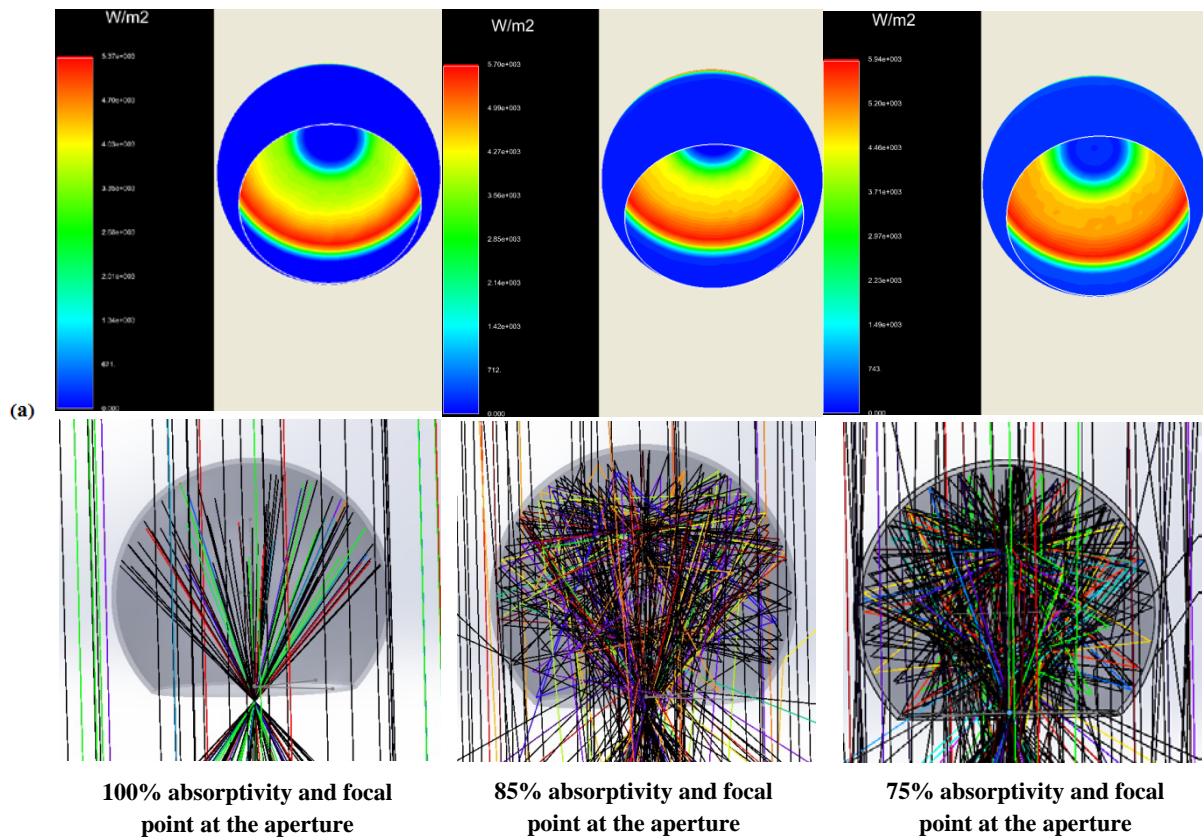**Fig. 6.** An example of initial simulations for the three different rim angle of parabolic concentrator.
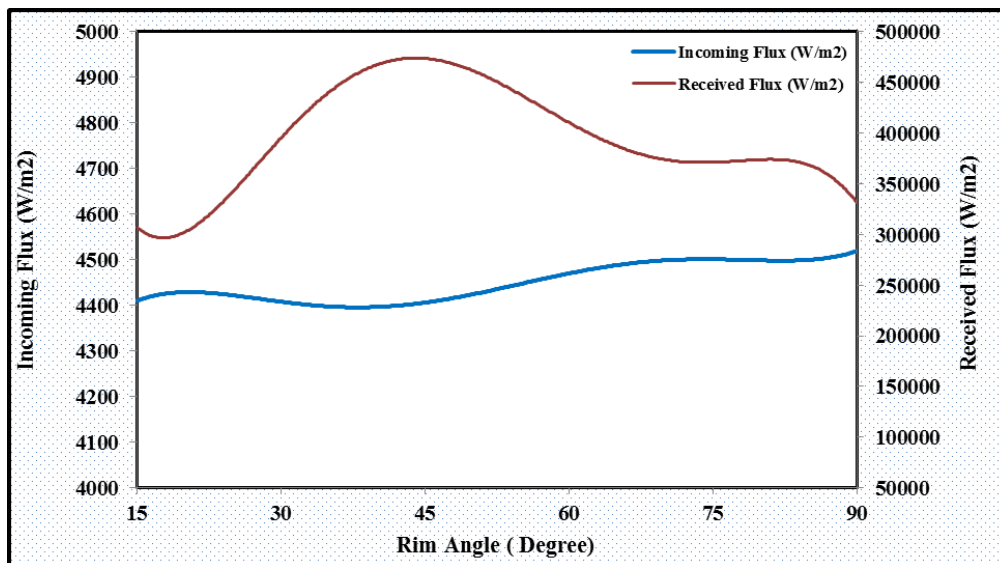
Fig. 7. Incoming and received flux at different concentrator rim angles.
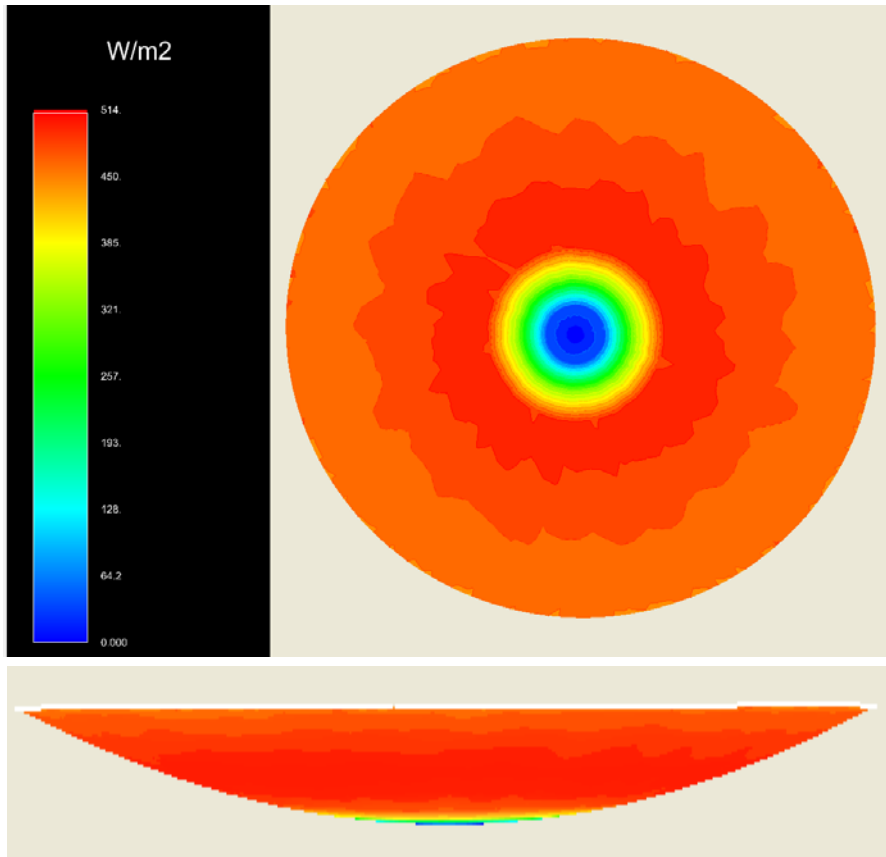
Fig. 8. An example of the 3D detector which was chosen in the studied parabolic concentrator shape.


(a)

| 100% absorptivity and focal point at the aperture | 85% absorptivity and focal point at the aperture | 75% absorptivity and focal point at the aperture |

(b)

| 100% absorptivity and focal point at the aperture | 85% absorptivity and focal point at the aperture | 75% absorptivity and focal point at the aperture |

(c)

| 100% absorptivity and Focal point at the aperture | 85% absorptivity and Focal point at the aperture | 75% absorptivity and Focal point at the aperture |

Fig. 9. The effect of absorptivity on the rays and flux distribution of (a) Spherical shape, (b) Conical shape and (c) Cylindrical shape.
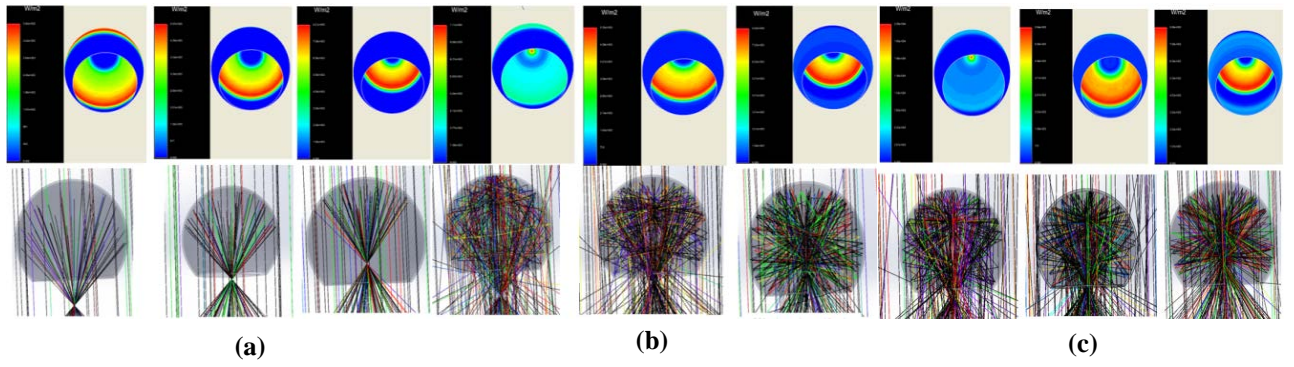
Fig. 10. The effect of receiver position on the rays and flux distributions for;
(a) 100%, (b) 85% and (c) 75% absorptivity.
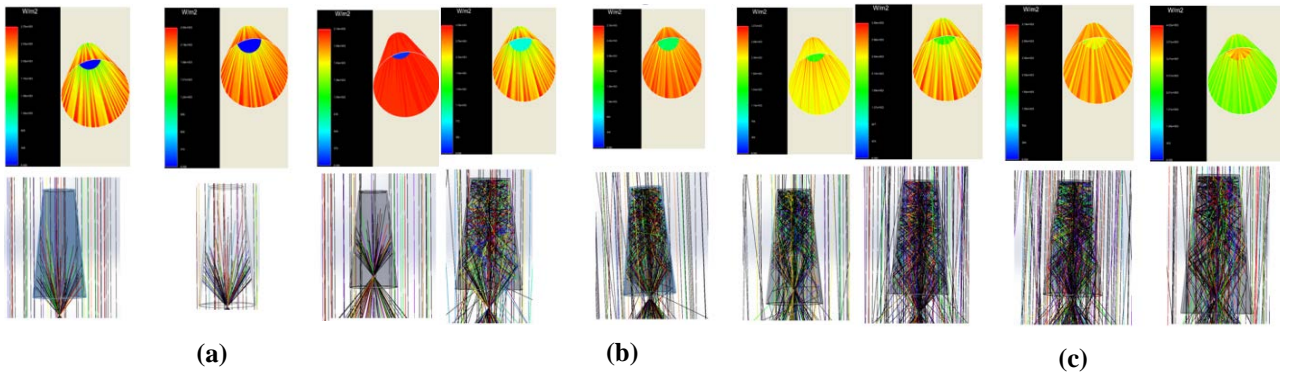
Fig. 11. The effect of receiver position on the rays and flux distributions for;
(a) 100%, (b) 85% and (c) 75% absorptivity.
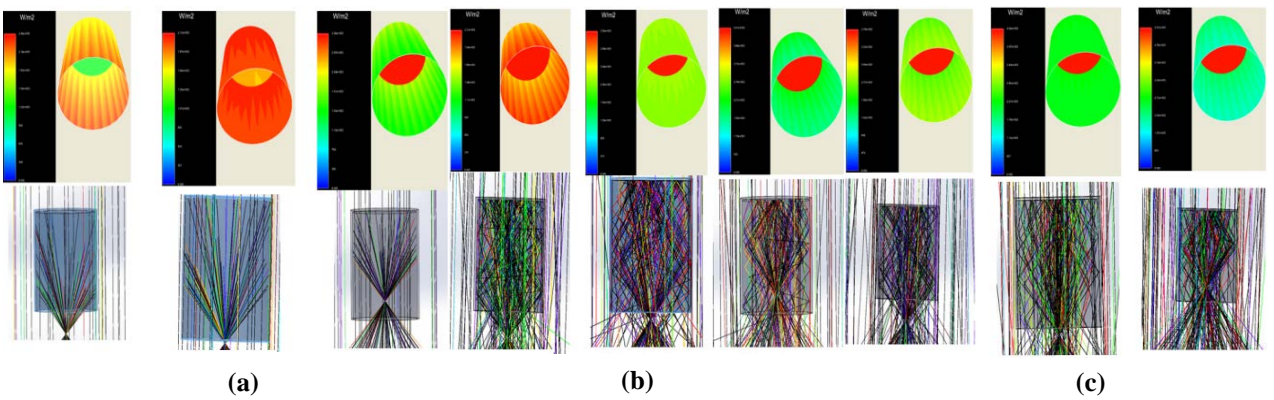
Fig. 12. The effect of receiver position on the rays and flux distributions for;
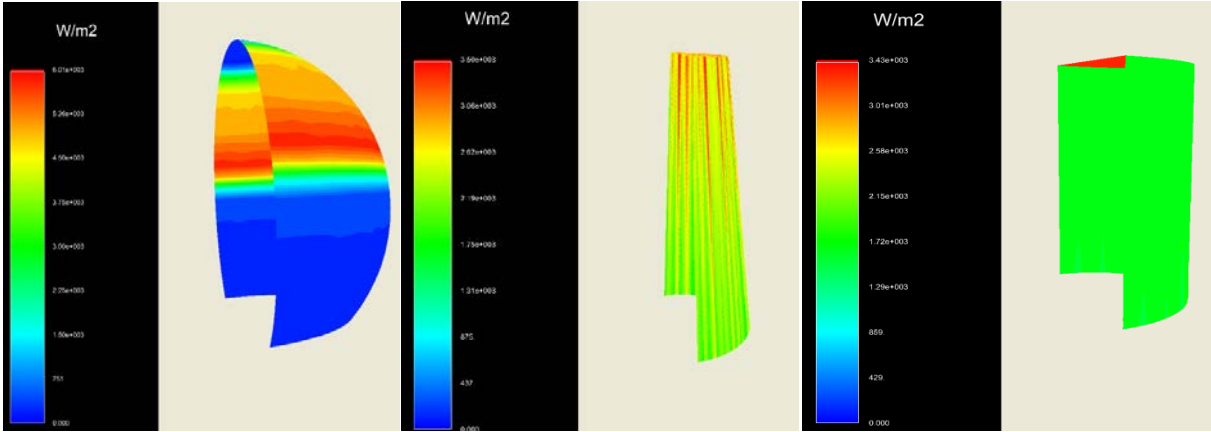(a) 100%, (b) 85% and (c) 75% absorptivity.

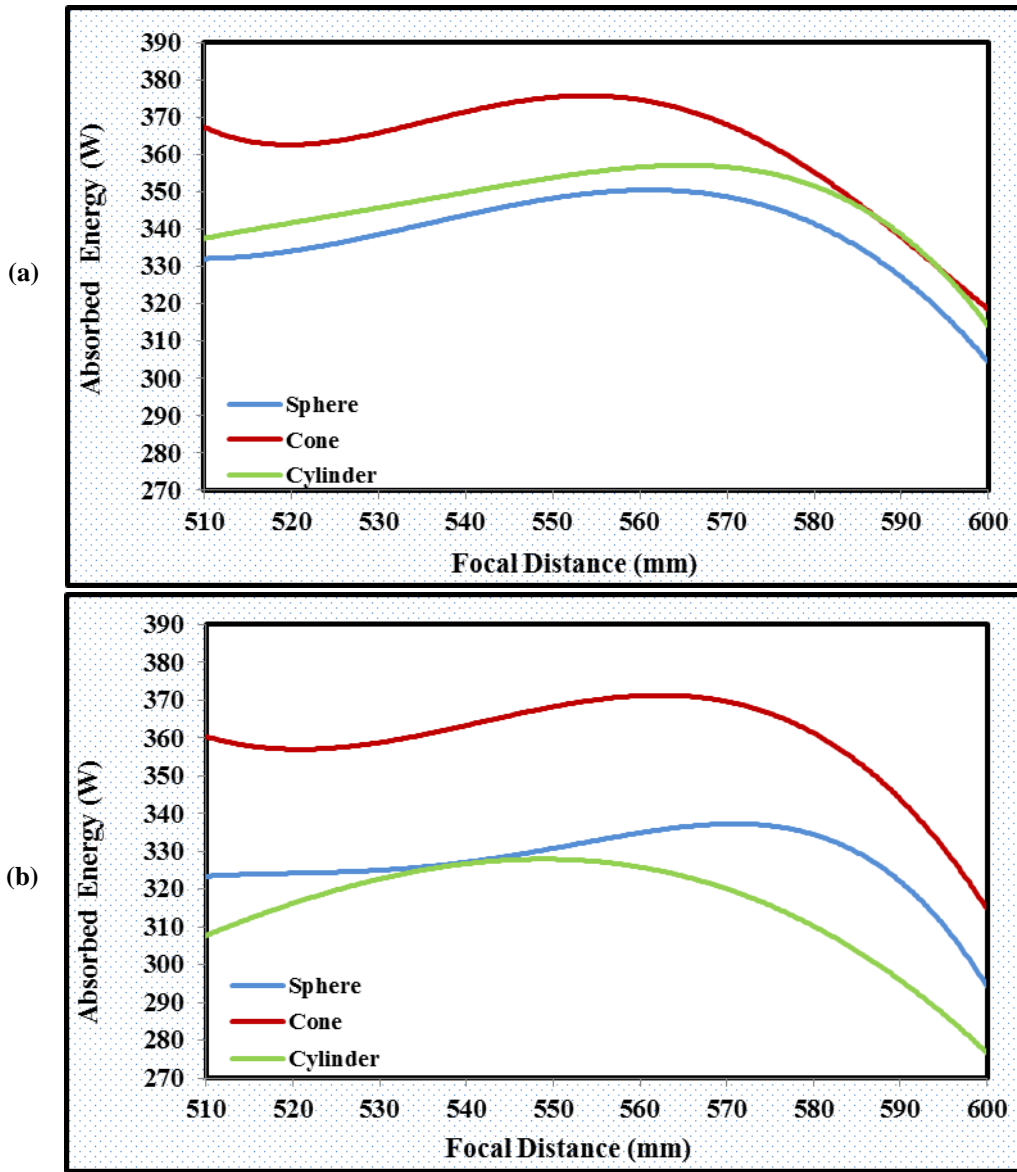**Fig. 13.** An enlarged cross sectional view for three receiver shapes.

Fig. 14. Absorbed energy for the three cavity receivers at different receiver positions and absorptivity of; (a) 85% and (b) 75%.
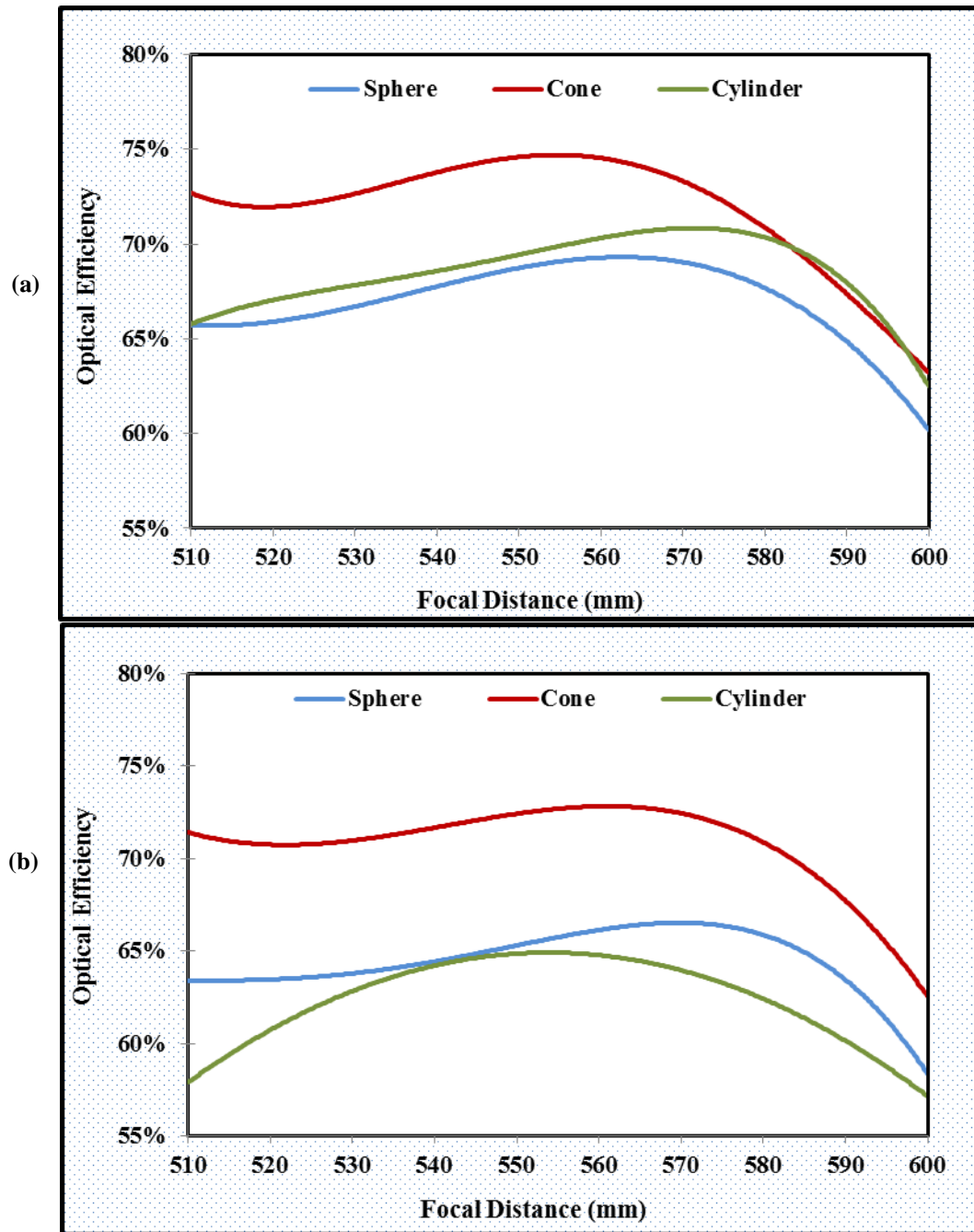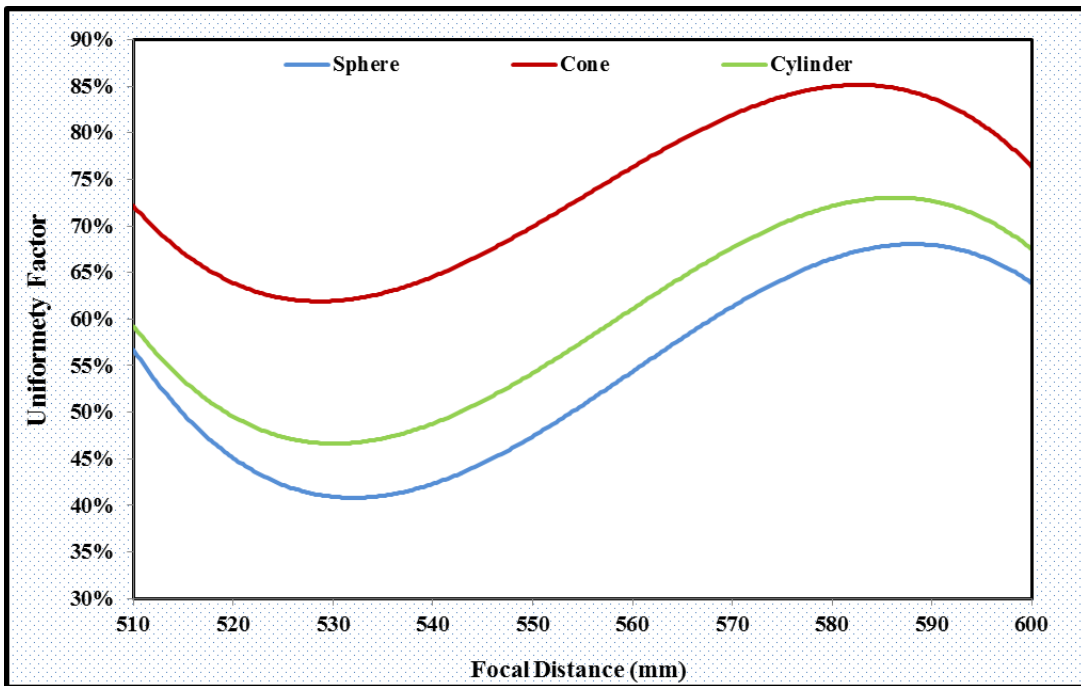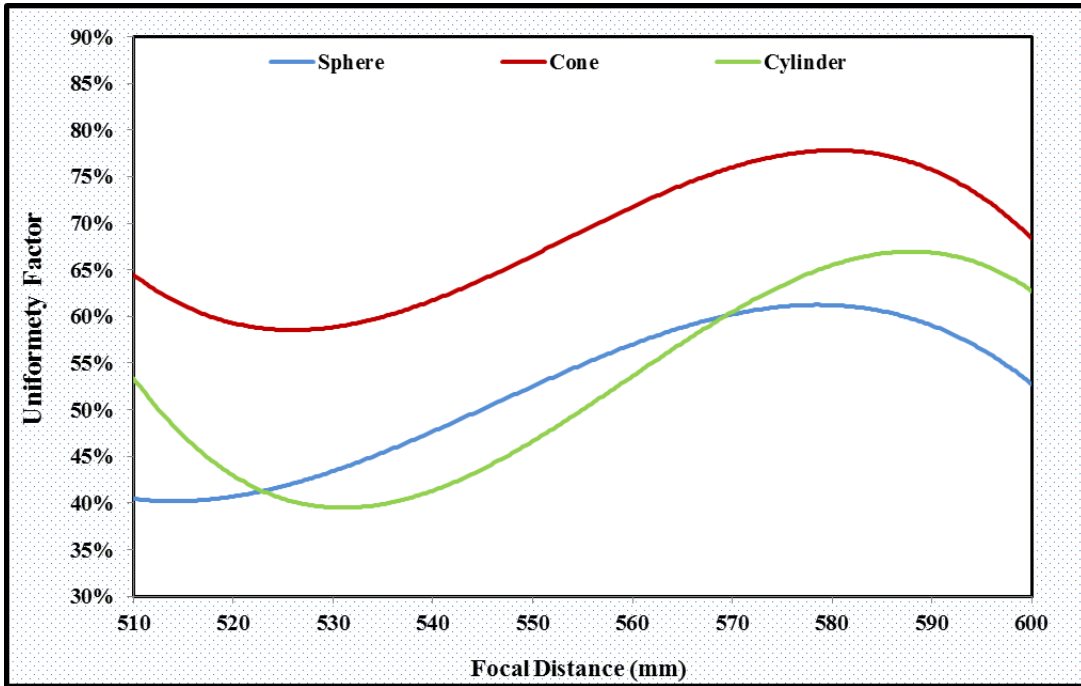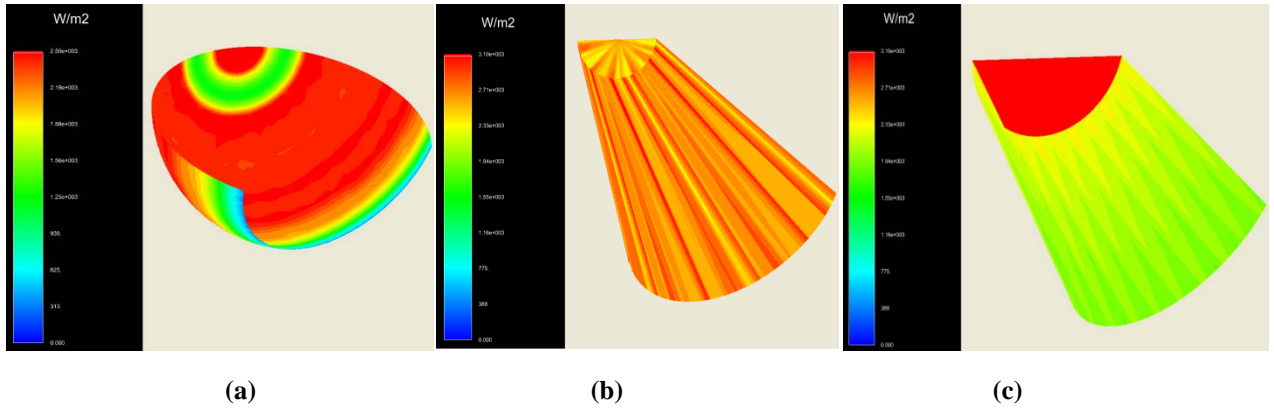
Fig. 15. Optical efficiency for the three cavity receivers at different receiver positions (mm) and absorptivity of; (a) 85% and (b) 75%.

Fig. 16. The illumination uniformity factor of the three cavity receivers at different receiver positions (mm) and absorptivity of; (a) 85% and (b) 75%.

Fig. 17. The best flux distributions of; (a) Spherical shape, (b) Conical shape and (c) Cylindrical shape.

Table 1: Dimensions of the parabolic concentrator and the three receivers				
Parameter	**Parabolic Concentrator**	**Cylindrical**	**Conical**	**Spherical**
ED (m)	1	0.20	0.20	0.20
T (m)	0.01	0.005	0.005	0.005
H (m)	0.1041	0.2499	0.3543	0.218